Physics Letters B 739 (2014) 218–228

Contents lists available at ScienceDirect

Physics Letters B

www.elsevier.com/locate/physletb

Measurement of the $\overline{B}^0$–B^0 and $\overline{B}^0_s$–B^0_s production asymmetries in pp collisions at $\sqrt{s} = 7$ TeV

LHCb Collaboration

ARTICLE INFO

Article history:
Received 1 August 2014
Received in revised form 23 September 2014
Accepted 1 October 2014
Available online 31 October 2014
Editor: L. Rolandi

ABSTRACT

The $\overline{B}^0$–B^0 and $\overline{B}^0_s$–B^0_s production asymmetries, $A_P(B^0)$ and $A_P(B^0_s)$, are measured by means of a time-dependent analysis of $B^0 \to J/\psi K^{*0}$, $B^0 \to D^-\pi^+$ and $B^0_s \to D^-_s\pi^+$ decays, using a data sample corresponding to an integrated luminosity of 1.0 fb^{-1}, collected by LHCb in pp collisions at a centre-of-mass energy of 7 TeV. The measurements are performed as a function of transverse momentum and pseudorapidity of the B^0 and B^0_s mesons within the LHCb acceptance. The production asymmetries, integrated over p_T and η in the range $4 < p_T < 30$ GeV/c and $2.5 < \eta < 4.5$, are determined to be $A_P(B^0) = (-0.35 \pm 0.76 \pm 0.28)\%$ and $A_P(B^0_s) = (1.09 \pm 2.61 \pm 0.66)\%$, where the first uncertainties are statistical and the second systematic.

1. Introduction

The production rates of b and $\bar{b}$ hadrons in pp collisions are not expected to be identical. This phenomenon, commonly referred to as the production asymmetry, is related to the fact that there can be coalescence between a perturbatively produced b or $\bar{b}$ quark and the u and d valence quarks in the beam remnant. Therefore, one can expect a slight excess in the production of B^+ and B^0 mesons with respect to B^- and $\overline{B}^0$ mesons, and *e.g.* of Λ^0_b baryons with respect to $\overline{\Lambda}^0_b$ baryons. As b and $\bar{b}$ quarks are almost entirely produced in pairs via strong interactions, the existence of B^+ and B^0 production asymmetries must be compensated by opposite production asymmetries for other B-meson and b-baryon species. These asymmetries are roughly estimated to be at the 1% level for pp collisions at LHC energies, and are expected to be enhanced at forward rapidities and small transverse momenta. Other subtle effects of quantum chromodynamics, beyond the coalescence between beauty quarks and light valence quarks, may also contribute [1–3].

The production asymmetry is one of the key ingredients to perform measurements of CP violation in b-hadron decays at the LHC, since CP asymmetries must be disentangled from other sources. The production asymmetry for B^0 and B^0_s mesons is defined as

$$A_P\left(B^0_{(s)}\right) \equiv \frac{\sigma(\overline{B}^0_{(s)}) - \sigma(B^0_{(s)})}{\sigma(\overline{B}^0_{(s)}) + \sigma(B^0_{(s)})}, \tag{1}$$

where σ denotes the production cross-section. Similar asymmetries are also expected when producing charmed hadrons. LHCb has already performed measurements of $D^+ - D^-$ and $D^+_s - D^-_s$ production asymmetries, finding values around the 1% level or less [4,5].

In this paper, the values of $A_P(B^0)$ and $A_P(B^0_s)$ are constrained by measuring the oscillations of B^0 and B^0_s mesons with a time-dependent analysis of the $B^0 \to J/\psi(\mu^+\mu^-)K^{*0}(K^+\pi^-)$, $B^0 \to D^-(K^+\pi^-\pi^-)\pi^+$ and $B^0_s \to D^-_s(K^+K^-\pi^-)\pi^+$ decay rates, without tagging the initial flavour of the decaying $B^0_{(s)}$ meson. The inclusion of charge-conjugate decay modes is implied throughout. The measurements are performed as a function of transverse momentum, p_T, and pseudorapidity, η, of the $B^0_{(s)}$ meson within the LHCb acceptance, and then integrated over the range $4 < p_T < 30$ GeV/c and $2.5 < \eta < 4.5$.

2. Detector, trigger and simulation

The LHCb detector [6] is a single-arm forward spectrometer covering the pseudorapidity range $2 < \eta < 5$, designed for the study of particles containing b or c quarks. The detector includes a high-precision tracking system consisting of a silicon-strip vertex detector surrounding the pp interaction region, a large-area silicon-strip detector located upstream of a dipole magnet with a bending power of about 4 Tm, and three stations of silicon-strip detectors and straw drift tubes placed downstream of the magnet. The tracking system provides a measurement of momentum with a relative uncertainty that varies from 0.4% at low momentum to 0.6% at 100 GeV/c. The minimum distance of a track to a primary vertex (PV), the impact parameter, is measured with

http://dx.doi.org/10.1016/j.physletb.2014.10.005

a resolution of $(15 + 29/p_T)$ μm, where p_T is in GeV/c. Different types of charged hadrons are distinguished using information from two ring-imaging Cherenkov detectors. Photon, electron and hadron candidates are identified by a calorimeter system consisting of scintillating-pad and preshower detectors, an electromagnetic calorimeter and a hadronic calorimeter. Muons are identified by a system composed of alternating layers of iron and multiwire proportional chambers. The trigger consists of a hardware stage, based on information from the calorimeter and muon systems, followed by a software stage, which applies a full event reconstruction.

In the case of the $B^0 \to J/\psi K^{*0}$ decay, events are first selected by a hardware trigger that requires muon candidates with $p_T > 1.48$ GeV/c. The subsequent software trigger is composed of two stages. The first stage performs a partial event reconstruction and requires events to have two well identified oppositely charged muons, with invariant mass larger than 2.7 GeV/c^2. The second stage performs a full event reconstruction and only retains events containing a $\mu^+\mu^-$ pair that has invariant mass within 120 MeV/c^2 of the known J/ψ mass [7] and forms a vertex that is significantly displaced from the nearest PV.

In the case of $B^0 \to D^-\pi^+$ and $B_s^0 \to D_s^-\pi^+$ decays, events are first selected by a hardware trigger requiring a high transverse energy cluster in the calorimeter system. Events passing the hardware trigger are further filtered by a software trigger which requires a two-, three- or four-track secondary vertex with a large sum of p_T of the tracks and a significant displacement from the PVs. Subsequently, a multivariate algorithm [8] is applied, aimed at identifying secondary vertices, consistent with the decay of a b hadron.

Simulated events are used to determine the signal selection efficiency, acceptance as function of decay time, decay time resolution, and to model the background. In the simulation, pp collisions are generated using Pythia 6.4 [9] with a specific LHCb configuration [10]. The interaction of the generated particles with the detector, and its response, are implemented using the Geant4 toolkit [11] as described in Ref. [12].

3. Data set and selection

The selection of $B^0 \to J/\psi K^{*0}$ candidates is based on the reconstruction of $J/\psi \to \mu^+\mu^-$ and $K^{*0} \to K^+\pi^-$ decays. The J/ψ candidates are formed from two oppositely charged tracks, identified as muons, having $p_T > 500$ MeV/c and originating from a common vertex. The invariant mass of this pair of muons must lie in the range 3030–3150 MeV/c^2. The K^{*0} candidates are formed from two oppositely charged tracks, one identified as a kaon and the other as a pion, originating from a common vertex. It is required that the K^{*0} candidate has $p_T > 1$ GeV/c and that the invariant mass lies in the range 826–966 MeV/c^2.

The B^0 candidates are reconstructed from the J/ψ and K^{*0} candidates, with the invariant mass of the $\mu^+\mu^-$ pair constrained to the known J/ψ mass. They are required to have an invariant mass in the range 5150–5400 MeV/c^2. The decay time of the B^0 candidate is calculated from a vertex and kinematic fit that constrains the candidate to originate from its associated PV [13]. The χ^2 per degree of freedom of the fit is required to be less than 10. Only B^0 candidates with a decay time greater than 0.2 ps are retained. This lower bound on the decay time rejects a large fraction of the prompt combinatorial background.

In the case of $B^0 \to D^-\pi^+$ and $B_s^0 \to D_s^-\pi^+$ decays, the selection of the B-meson candidate is based on the reconstruction of $D^- \to K^+\pi^-\pi^-$ and $D_s^- \to K^+K^-\pi^-$ decays, respectively. Requirements are made on the $D_{(s)}^-$ decay products before combining them to form a common vertex. The scalar p_T sum of the tracks must exceed 1.8 GeV/c and the maximal distance of closest approach between all possible pairs of tracks must be less than 0.5 mm. The $D_{(s)}^-$ candidate is required to have a significant flight distance with respect to the associated PV, by requiring a χ^2 greater than 36 compared to the zero distance hypothesis. The masses of the D^- and D_s^- candidates must lie within 1850–1890 MeV/c^2 and 1949–1989 MeV/c^2, respectively. They are subsequently combined with a fourth particle, the bachelor pion, to form the B-meson decay vertices. The sum of the $D_{(s)}^-$ and bachelor pion p_T values must be larger than 5 GeV/c and the decay time of B-meson candidates must be greater than 0.2 ps. The cosine of the angle between the B-meson candidate momentum vector and the line segment between the PV and B-meson candidate vertex is required to be larger than 0.999. Particle identification (PID) selection criteria are applied to the kaons and pions from the $D_{(s)}^-$ candidate, and to the bachelor pion, in order to reduce the background from other B-meson decays with a misidentified kaon or pion and from Λ_b^0 decays with a misidentified proton to a negligible level.

A final selection is applied to the candidates that satisfy the criteria described above. It uses a multivariate analysis method [14,15], optimized separately for each of the three decay modes, to reject the combinatorial background. The variables used in the selection for the B decay products are the transverse momentum and the impact parameter. For the B candidates the variables employed are the transverse momentum, the distance of flight and the impact parameter.

4. Fit model

For each signal and background component, the distributions of invariant mass and decay time of B-meson candidates are modelled by appropriate probability density functions (PDFs). We consider two categories of background: the combinatorial background, due to the random association of tracks, and the partially reconstructed background, due to decays with a topology similar to that of the signal, but with one or more particles not reconstructed. The latter is present only for $B_{(s)}^0 \to D_{(s)}^-\pi^+$ decays.

4.1. Mass model

The signal component for each decay is modelled convolving a double Gaussian function with a function parameterizing the final state radiation. The PDF of the B invariant mass, m, is given by

$$g(m) = A\left[\Theta(\mu - m)(\mu - m)\right]^s \otimes G(m), \tag{2}$$

where A is a normalization factor, Θ is the Heaviside function, G is the sum of two Gaussian functions with different widths and zero mean, and μ is the B meson mass. The parameter $s \simeq -0.99$ governs the amount of final state radiation, and is determined using simulated events for each of the three decay modes. The combinatorial background is modelled by an exponential function for all final states. In the case of $B^0 \to D^-\pi^+$ and $B_s^0 \to D_s^-\pi^+$ decays, a background component due to partially reconstructed B^0 and B_s^0 decays is also present in the low invariant mass region. The main contributions are expected to come from decays with a missing γ or π^0: $B^0 \to D^{*-}(D^-\gamma, D^-\pi^0)\pi^+$ decays with $D^- \to K^+\pi^-\pi^-$; $B^0 \to D^-(K^+\pi^-\pi^-)\rho^+(\pi^+\pi^0)$ decays; $B_s^0 \to D_s^{*-}(D_s^-\gamma, D_s^-\pi^0)\pi^+$ decays with $D_s^- \to K^+K^-\pi^-$; $B_s^0 \to D_s^-(K^+K^-\pi^-)\rho^+(\pi^+\pi^0)$ decays.

We parameterize the partially reconstructed components by means of a kernel estimation technique [16] based on invariant mass distributions obtained from full simulation, using the same selection as for data. In the case of $B_s^0 \to D_s^-\pi^+$ decays, there

is also a background component due to $B^0 \to D_s^+\pi^-$ decays. We account for this component in the fits using the same parameterization adopted for the signal. The $B^0 \to D_s^+\pi^-$ yield is fixed using the ratio between hadronization fractions measured by LHCb [17,18] and the world average of branching fractions [7].

4.2. Decay time model

The time-dependent decay rate of a neutral $B^0_{(s)}$ or $\overline{B}{}^0_{(s)}$ meson to a flavour-specific f or $\bar{f}$ final state is given by the PDF

$$h(t,\psi) = K(1-\psi A_{CP})(1-\psi A_f) \times \left\{ e^{-\Gamma t}\left[\Lambda_+ \cosh\left(\frac{\Delta\Gamma t}{2}\right) + \psi\Lambda_- \cos(\Delta m t)\right]\right\} \otimes R(t)\epsilon(t), \quad (3)$$

where K is a normalization factor, $\epsilon(t)$ is the acceptance as a function of the decay time, $R(t)$ is the decay time resolution function, $\Delta m \equiv m_{\rm H} - m_{\rm L}$ and $\Delta\Gamma \equiv \Gamma_{\rm L} - \Gamma_{\rm H}$ are the mass and decay-width differences of the $B^0_{(s)} - \overline{B}{}^0_{(s)}$ system mass eigenstates and Γ is the average decay width. The subscripts H and L denote the heavy and light eigenstates, respectively. The two observables are the decay time t and the tag of the final state ψ, which assumes the values $\psi = 1$ if the final state is f and $\psi = -1$ if the final state is the CP conjugate $\bar{f}$. The terms Λ_+ and Λ_- are defined as

$$\Lambda_\pm \equiv (1 - A_{\rm P})\left|\frac{q}{p}\right|^{1-\psi} \pm (1 + A_{\rm P})\left|\frac{q}{p}\right|^{-1-\psi}, \quad (4)$$

where p and q are complex parameters entering the definition of the two mass eigenstates of the effective Hamiltonian in the $B^0_{(s)}$ system, $p|B^0_{(s)}\rangle \pm q|\overline{B}{}^0_{(s)}\rangle$. The symbol $A_{\rm P}$ denotes the production asymmetry of the given B meson, and A_f is the detection asymmetry of the final state, defined in terms of the f and $\bar{f}$ detection efficiencies as

$$A_f \equiv \frac{\epsilon_{\bar{f}} - \epsilon_f}{\epsilon_{\bar{f}} + \epsilon_f}. \quad (5)$$

The direct CP asymmetry A_{CP} is defined as

$$A_{CP} \equiv \frac{\mathcal{B}(\overline{B}{}^0_{(s)} \to \bar{f}) - \mathcal{B}(B^0_{(s)} \to f)}{\mathcal{B}(\overline{B}{}^0_{(s)} \to \bar{f}) + \mathcal{B}(B^0_{(s)} \to f)}. \quad (6)$$

Trigger and event selections lead to distortions in the shapes of the decay time distributions. The signal decay time acceptances are determined from simulated events. For each simulated decay we apply trigger and selection algorithms as in real data.

Concerning the combinatorial and the partially reconstructed backgrounds, empirical parameterizations of the decay time spectra are determined by studying the low and high invariant mass sidebands from data. Partially reconstructed backgrounds are only present in the case of $B^0 \to D^-\pi^+$ and $B_s^0 \to D_s^-\pi^+$ decays. In the case of $B_s^0 \to D_s^-\pi^+$ decays, the additional background component due to $B^0 \to D_s^+\pi^-$ decays is modelled using the same functional form as that of the $B_s^0 \to D_s^-\pi^+$ signal, and the value of the production asymmetry is fixed to that obtained from the $B^0 \to D^-\pi^+$ fit.

4.3. Decay time resolution

The strategy adopted to study the decay time resolution of the detector consists of reconstructing the decay time of fake B candidates formed from a D^- decaying to $K^+\pi^-\pi^-$ and a pion track, both coming from the same PV. The bachelor pion must be selected without introducing biases on the decay time, hence only requirements on momentum and transverse momentum are applied, avoiding the use of impact parameter variables. The decay time distribution of these fake B candidates yields an estimate of the decay time resolution of a real decay. In order to validate the method, simulated events are used for both signals and fake B decays. The resolution is found to be overestimated by about 4 fs. This difference is taken into account as a systematic effect. The simulation also indicates that a dependence of the resolution on the decay time must be considered. Taking this into account, an average decay time resolution of 49 ± 8 fs is estimated. A resolution model, $R(t)$, consisting of a triple Gaussian function with zero mean and three different widths, characterized by an average width of 49 fs, is used. The uncertainty of 8 fs on the average width is taken into account as a systematic uncertainty. It is estimated from simulation that the measurement of the decay time is biased by no more than 2 fs, and the effect is accounted for as a systematic uncertainty.

Table 1
Values of the various physical inputs used in the fits.

Parameter	Value	Reference
Δm_d [ps^{-1}]	0.510 ± 0.004	[7]
Δm_s [ps^{-1}]	17.768 ± 0.024	[19]
Γ_d [ps^{-1}]	0.6583 ± 0.0030	[7]
Γ_s [ps^{-1}]	0.6596 ± 0.0046	[7]
$\Delta\Gamma_s$ [ps^{-1}]	0.081 ± 0.011	[7]
$\lvert q/p\rvert_{B^0}$	0.9997 ± 0.0013	[20]
$\lvert q/p\rvert_{B_s^0}$	1.0003 ± 0.0030	[21]

5. Determination of the production asymmetries

The production asymmetry for each of the three decay modes is determined by means of a simultaneous fit to the invariant mass and decay time spectra. To account for the dependence of the production asymmetries on the kinematics of the B^0 and B_s^0 mesons, each data sample must be divided into bins of $(p_{\rm T}, \eta)$, performing the same fit for each bin.

In order to validate the fit model, a series of fits to the distributions of events obtained from fast simulations is used to verify the accuracy of the central values and the reliability of the uncertainties. No evidence of biases on central values nor of uncertainty misestimations is found. Furthermore, a global fit to the total sample of selected events is performed for each of the three decay modes. The mass differences Δm_d and Δm_s, the mixing parameters $|q/p|_{B^0}$ and $|q/p|_{B_s^0}$, the average decay widths Γ_d and Γ_s, and the width difference $\Delta\Gamma_s$ are fixed to the central values of the measurements reported in Table 1. The width difference $\Delta\Gamma_d$ is fixed to zero.

According to Eq. (3), for small values of A_{CP} and A_f, to first order the decay rate is only sensitive to the sum of these two quantities. For this reason, we fix A_{CP} to zero and leave A_f as a free parameter in the fits. It is empirically verified that the choice of different A_{CP} values, up to the few percent level, leads to negligible variations of $A_{\rm P}$, as expected.

Fig. 1 shows the $J/\psi K^+\pi^-$, $K^+\pi^-\pi^-\pi^+$ and $K^+K^-\pi^-\pi^+$ invariant mass and decay time distributions, with the results of the global fits overlaid. Fig. 2 shows the raw asymmetries, defined as the ratios between the difference and the sum of the overall decay time distributions, as a function of decay time for candidates in the signal mass region. The signal yields, $A_{\rm P}$ values and detection asymmetries obtained from the global fits are reported in Table 2. The $A_{\rm P}$ values obtained from the global fits are not well defined physical quantities, because efficiency corrections as a function of

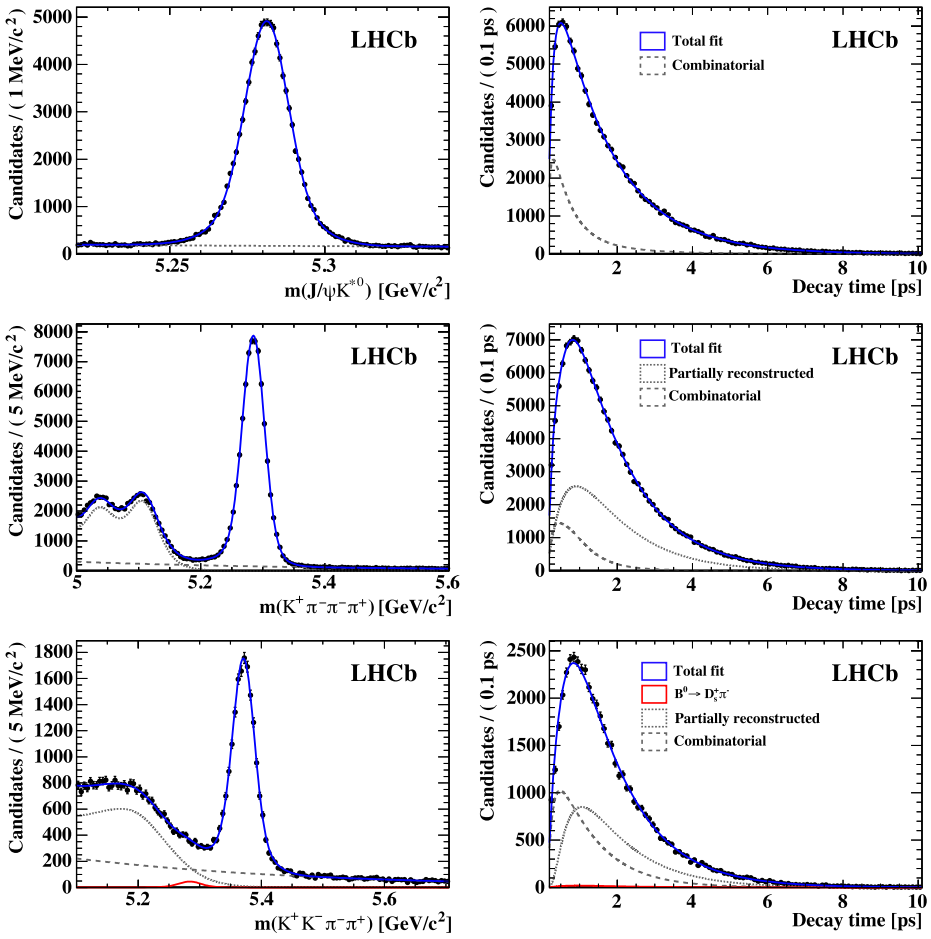

Fig. 1. Distributions of (left) invariant mass and (right) decay time for (top) $B^0 \to J/\psi K^{*0}$, (middle) $B^0 \to D^-\pi^+$ and (bottom) $B_s^0 \to D_s^-\pi^+$ decays, with the results of the fit overlaid. The contributions of the various background sources are also shown.

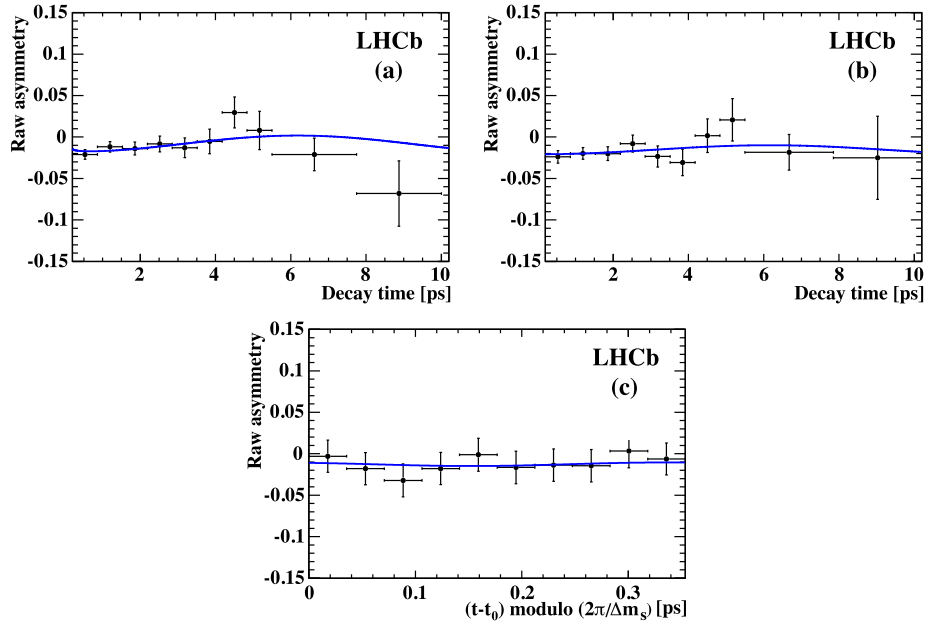

Fig. 2. Time-dependent raw asymmetries for candidates in the (a) $B^0 \to J/\psi K^{*0}$, (b) $B^0 \to D^-\pi^+$ and (c) $B_s^0 \to D_s^-\pi^+$ signal mass regions with the results of the global fits overlaid. In (c) the asymmetry is obtained by folding the $\overline{B}_s^0$ and B_s^0 decay time distributions into one oscillation period, and the offset $t_0 = 0.2$ ps corresponds to the selection requirement on the decay time.

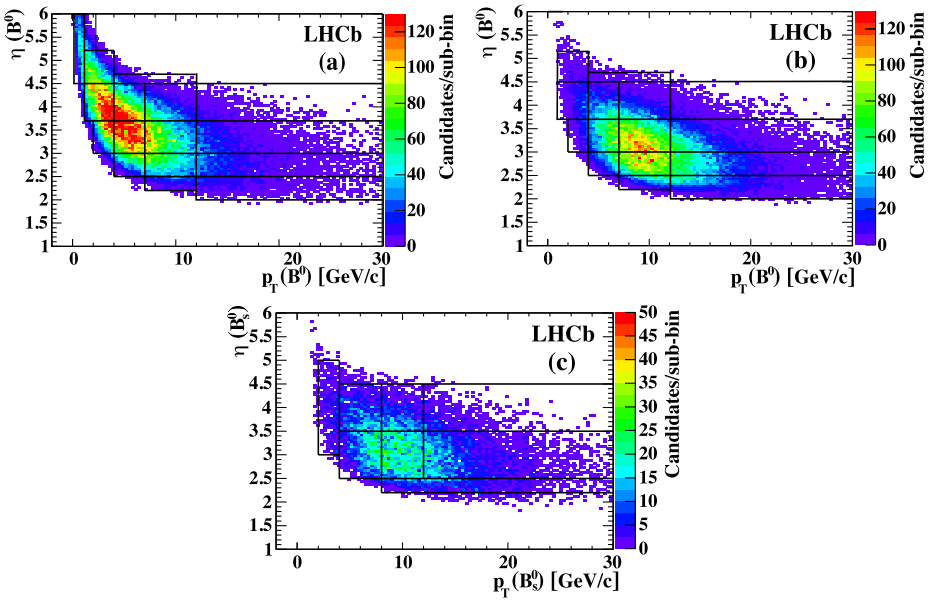

Fig. 3. Distributions of p_{T} and η, where the background components are subtracted using the *sPlot* technique [22], for (a) $B^0 \to J/\psi K^{*0}$, (b) $B^0 \to D^-\pi^+$ and (c) $B_s^0 \to D_s^-\pi^+$ decays. The definition of the various kinematic bins is superimposed.

Table 2
Values of signal yields, A_{P}, A_f and of the correlations $\rho(A_{\mathrm{P}}, A_f)$ obtained from global fits. The smaller value of the correlation in the B_s^0 case is due to the much larger mixing frequency of B_s^0 mesons.

Parameter	$B^0 \to J/\psi K^{*0}$	$B^0 \to D^-\pi^+$	$B_s^0 \to D_s^-\pi^+$
N^{sig}	$93\,627 \pm 360$	$76\,682 \pm 308$	$16\,887 \pm 174$
A_{P}	-0.0116 ± 0.0063	-0.0058 ± 0.0070	-0.0032 ± 0.0166
A_f	-0.0086 ± 0.0046	-0.0151 ± 0.0049	-0.0110 ± 0.0086
$\rho(A_{\mathrm{P}}, A_f)$	-0.65	-0.64	-0.01

p_{T} and η need to be applied. They are reported here for illustrative purposes only.

Fig. 3 shows the two-dimensional distributions of (p_{T}, η) for $B^0 \to J/\psi K^{*0}$, $B^0 \to D^-\pi^+$ and $B_s^0 \to D_s^-\pi^+$ decays. The background components are subtracted using the *sPlot* technique [22] and the chosen definition of the various kinematic bins is overlaid. For the two B^0 decays we use a common set of bins, as reported in Table 3, in order to allow a simple combination of the two independent A_{P} measurements. In the case of the $B^0 \to J/\psi K^{*0}$, two additional bins at small p_{T} and large η are also defined. An accurate knowledge of the decay time resolution is important for $B_s^0 \to D_s^-\pi^+$ decay, due to the fast oscillation of the B_s^0 meson. For this reason we determine the decay time resolution using the method previously described, applied to events belonging to each (p_{T}, η) bin, where a double Gaussian function with zero mean and values of the widths depending on the given bin is used.

6. Systematic uncertainties

Several sources of systematic uncertainty that affect the determination of the production asymmetries are considered. For the invariant mass model, the effects of the uncertainty on the shapes of all components (signals, combinatorial and partially reconstructed backgrounds) are investigated. For the decay time model, systematic effects related to the decay time resolution and acceptance are studied. The effects of the uncertainties on the external inputs used in the fits, reported in Table 1, are evaluated by repeating the fits with each parameter varied by $\pm 1\sigma$. Alternative parameteriza-

Table 3
Combined values of $A_{\mathrm{P}}(B^0)$ from $B^0 \to J/\psi K^{*0}$ and $B^0 \to D^-\pi^+$ decays, corresponding to the various kinematic bins. The first uncertainties are statistical and the second systematic. For completeness, the values obtained either from $B^0 \to J/\psi K^{*0}$ or $B^0 \to D^-\pi^+$ decays are also reported in the last two columns, with statistical uncertainties only. The values of the last two bins are obtained from $B^0 \to J/\psi K^{*0}$ decays alone.

p_{T} (GeV/c)	η	$A_{\mathrm{P}}(B^0)$	$A_{\mathrm{P}}(B^0 \to J/\psi K^{*0})$	$A_{\mathrm{P}}(B^0 \to D^-\pi^+)$
(1.0, 4.0)	(4.5, 5.2)	$0.0016 \pm 0.0253 \pm 0.0016$	0.0037 ± 0.0260	-0.0331 ± 0.1044
(1.0, 4.0)	(3.7, 4.5)	$-0.0158 \pm 0.0162 \pm 0.0015$	-0.0161 ± 0.0170	-0.0130 ± 0.0519
(2.0, 4.0)	(3.0, 3.7)	$0.0055 \pm 0.0254 \pm 0.0016$	0.0078 ± 0.0271	-0.0114 ± 0.0738
(4.0, 12.0)	(4.5, 4.7)	$0.0160 \pm 0.0736 \pm 0.0067$	-0.0489 ± 0.0840	0.2353 ± 0.1529
(4.0, 7.0)	(3.7, 4.5)	$-0.0189 \pm 0.0158 \pm 0.0032$	-0.0221 ± 0.0184	-0.0099 ± 0.0310
(4.0, 7.0)	(3.0, 3.7)	$-0.0311 \pm 0.0132 \pm 0.0014$	-0.0342 ± 0.0160	-0.0245 ± 0.0232
(4.0, 7.0)	(2.5, 3.0)	$0.0556 \pm 0.0254 \pm 0.0020$	0.0703 ± 0.0324	0.0321 ± 0.0408
(7.0, 12.0)	(3.7, 4.5)	$-0.0145 \pm 0.0205 \pm 0.0027$	-0.0364 ± 0.0269	0.0161 ± 0.0316
(7.0, 12.0)	(3.0, 3.7)	$-0.0142 \pm 0.0111 \pm 0.0015$	-0.0067 ± 0.0173	-0.0196 ± 0.0146
(7.0, 12.0)	(2.5, 3.0)	$-0.0236 \pm 0.0138 \pm 0.0014$	-0.0341 ± 0.0228	-0.0175 ± 0.0173
(7.0, 12.0)	(2.2, 2.5)	$-0.0190 \pm 0.0348 \pm 0.0034$	-0.0397 ± 0.0623	-0.0096 ± 0.0420
(12.0, 30.0)	(3.7, 4.5)	$-0.0550 \pm 0.0473 \pm 0.0020$	-0.0195 ± 0.0649	-0.0951 ± 0.0690
(12.0, 30.0)	(3.0, 3.7)	$0.0067 \pm 0.0180 \pm 0.0021$	-0.0193 ± 0.0311	0.0199 ± 0.0220
(12.0, 30.0)	(2.5, 3.0)	$0.0177 \pm 0.0162 \pm 0.0023$	0.0295 ± 0.0314	0.0134 ± 0.0190
(12.0, 30.0)	(2.0, 2.5)	$-0.0018 \pm 0.0236 \pm 0.0020$	0.0031 ± 0.0485	-0.0033 ± 0.0270
(0.2, 1.0)	(4.5, 6.0)	$-0.0391 \pm 0.0501 \pm 0.0016$	-0.0391 ± 0.0501	–
(1.0, 2.2)	(5.2, 6.0)	$0.0523 \pm 0.0684 \pm 0.0025$	0.0523 ± 0.0684	–

tions of the background components are also considered. To estimate the contribution of each single source, we repeat the fit for each (p_T, η) bin after having modified the baseline fit model. The shifts from the relevant baseline values are taken as the systematic uncertainties. To estimate a systematic uncertainty related to the parameterization of final state radiation effects on the signal mass distributions, the parameter s of Eq. (2) is varied by $\pm 1\sigma$ of the corresponding value obtained from fits to simulated events. A systematic uncertainty related to the invariant mass resolution model is estimated by repeating the fit using a single Gaussian function. The systematic uncertainty related to the parameterization of the mass shape for the combinatorial background is investigated by replacing the exponential function with a straight line. Concerning the partially reconstructed background, we assess a systematic uncertainty by repeating the fits while excluding the low mass sideband, *i.e.* applying the requirements $m > 5.20$ GeV/c^2 for the $B^0 \to D^-\pi^+$ decays and $m > 5.33$ GeV/c^2 for $B^0_s \to D^-_s\pi^+$ decays. To estimate the uncertainty related to the parameterization of signal decay time acceptances, different acceptance functions are considered. Effects of inaccuracies in the knowledge of the decay time resolution are estimated by rescaling the widths of the baseline model to obtain an average resolution width differing by ± 8 fs. Simulation studies also indicate that there is a small bias in the reconstructed decay time. The impact of such a bias is assessed by introducing a corresponding bias of ± 2 fs in the decay time resolution model.

The determination of the systematic uncertainties related to the $|q/p|$ input value needs a special treatment, as A_P is correlated with $|q/p|$. For this reason, any variation of $|q/p|$ turns into the same shift of A_P in each of the kinematic bins. Such a correlation is taken into account when averaging $A_P(B^0)$ measurements from $B^0 \to J/\psi K^{*0}$ and $B^0 \to D^-\pi^+$ decays, or when integrating over p_T and η. The values of the systematic uncertainties related to the knowledge of $|q/p|$ are 0.0013 in the case of $A_P(B^0)$ and 0.0030 in the case of $A_P(B^0_s)$. The dominant systematic uncertainties for the $B^0 \to J/\psi K^{*0}$ decay are related to the signal mass shape and to $|q/p|$. For the $B^0 \to D^-\pi^+$ decay, the most relevant systematic uncertainties are related to the signal mass shape and to the partially reconstructed background. Systematic uncertainties associated with the decay time resolution and Δm_s are the main sources for the $B^0_s \to D^-_s\pi^+$ decay.

7. Results

The values of $A_P(B^0)$ are determined independently for $B^0 \to J/\psi K^{*0}$ and $B^0 \to D^-\pi^+$ decays in each kinematic bin and then averaged. Table 3 reports the final results. The overall bin-by-bin agreement between the two sets of independent $A_P(B^0)$ measurements is evaluated by means of a χ^2 test, with a $\chi^2 = 7$ for 14 degrees of freedom. The values of $A_P(B^0_s)$ determined from the $B^0_s \to D^-_s\pi^+$ fits are reported in Table 4.

The integration over p_T and η of the bin-by-bin A_P values is performed within the ranges $4 < p_T < 30$ GeV/c and $2.5 < \eta < 4.5$. The integrated value of A_P is given by

$$A_P = \frac{\sum_i \frac{N_i}{\varepsilon_i} A_{P,i}}{\sum_i \frac{N_i}{\varepsilon_i}}, \tag{7}$$

where the index i runs over the bins, N_i is the number of signal events and ε_i is the efficiency, defined as the number of selected events divided by the number of produced events in the i-th bin. The signal yield in each bin can be expressed as

$$N_i = \mathcal{L} \cdot \sigma_{b\bar{b}} \cdot 2 \cdot f_{d(s)} \cdot \mathcal{B} \cdot f_i \cdot \varepsilon_i, \tag{8}$$

Table 4
Values of $A_P(B^0_s)$ from $B^0_s \to D^-_s\pi^+$ decays, corresponding to the various kinematic bins. The first uncertainties are statistical and the second systematic.

p_T (GeV/c)	η	$A_P(B^0_s)$
(2, 4)	(3.0, 5.0)	$-0.1475 \pm 0.0895 \pm 0.0192$
(4, 8)	(3.5, 4.5)	$-0.0471 \pm 0.0513 \pm 0.0112$
(4, 8)	(2.5, 3.5)	$0.0376 \pm 0.0467 \pm 0.0083$
(8, 12)	(3.5, 4.5)	$0.0582 \pm 0.0537 \pm 0.0053$
(8, 12)	(2.5, 3.5)	$0.0370 \pm 0.0332 \pm 0.0051$
(12, 30)	(3.5, 4.5)	$-0.0339 \pm 0.0750 \pm 0.0095$
(12, 30)	(2.5, 3.5)	$-0.0333 \pm 0.0309 \pm 0.0040$
(8, 30)	(2.2, 2.5)	$-0.0351 \pm 0.0485 \pm 0.0059$

Table 5
Values of ω_i determined from simulation and ω_i^{data} extracted from data using $B^0 \to J/\psi K^{*0}$ decays in two different binning schemes. The ω_i values and the difference between ω_i and ω_i^{data} values are used to determine the integrated results and to evaluate the related systematic uncertainties, respectively.

p_T (GeV/c)	η	ω_i	ω_i^{data}
(4, 7)	(3.7, 4.5)	0.1698 ± 0.0008	0.1946 ± 0.0025
(4, 7)	(3.0, 3.7)	0.2432 ± 0.0009	0.2396 ± 0.0036
(4, 7)	(2.5, 3.0)	0.2222 ± 0.0009	0.1976 ± 0.0051
(7, 12)	(3.7, 4.5)	0.0662 ± 0.0006	0.0789 ± 0.0016
(7, 12)	(3.0, 3.7)	0.1129 ± 0.0007	0.1129 ± 0.0045
(7, 12)	(2.5, 3.0)	0.1150 ± 0.0007	0.1002 ± 0.0019
(12, 30)	(3.7, 4.5)	0.0113 ± 0.0003	0.0160 ± 0.0007
(12, 30)	(3.0, 3.7)	0.0276 ± 0.0004	0.0307 ± 0.0028
(12, 30)	(2.5, 3.0)	0.0318 ± 0.0004	0.0296 ± 0.0025
(4, 8)	(3.5, 4.5)	0.2667 ± 0.0009	0.3064 ± 0.0020
(4, 8)	(2.5, 3.5)	0.4766 ± 0.0009	0.4644 ± 0.0030
(8, 12)	(3.5, 4.5)	0.0564 ± 0.0005	0.0640 ± 0.0015
(8, 12)	(2.5, 3.5)	0.1295 ± 0.0008	0.0873 ± 0.0019
(12, 30)	(3.5, 4.5)	0.0175 ± 0.0003	0.0238 ± 0.0008
(12, 30)	(2.5, 3.5)	0.0532 ± 0.0005	0.0541 ± 0.0027

where $\mathcal{L}$ is the integrated luminosity, $\sigma_{b\bar{b}}$ is the $b\bar{b}$ cross section, $f_{d(s)}$ is the $B^0_{(s)}$ hadronization fraction, f_i is the fraction of B mesons produced in the i-th bin and $\mathcal{B}$ is the branching fraction of the B decay. By substituting N_i/ε_i from Eq. (8) into Eq. (7), the integrated value of A_P becomes

$$A_P = \sum_i \omega_i A_{P,i}, \tag{9}$$

where $\omega_i = f_i / \sum_i f_i$. The values of ω_i are determined using simulated events. The difference between the values of ω_i predicted by Pythia for B^0 and B^0_s mesons is found to be negligible, if the same bins in p_T and η would be used. These values are also extracted from data using $B^0 \to J/\psi K^{*0}$ decays. In this case ω_i^{data} is measured as

$$\omega_i^{\text{data}} = \frac{N_i}{\varepsilon_i^{\text{rec}}} \Big/ \sum_j \frac{N_j}{\varepsilon_j^{\text{rec}}}, \tag{10}$$

where N_i is the yield in the i-th bin and $\varepsilon_i^{\text{rec}}$ is total reconstruction efficiency. The values of $\varepsilon_i^{\text{rec}}$ are determined using both simulated events and data control samples. The values of ω_i and ω_i^{data}, summarized in Table 5, exhibit systematic differences at the 10% level. The difference in the central value between $A_P(B^0 \to J/\psi K^{*0})$ calculated using either ω_i or ω_i^{data} is found to be 0.0024 using the B^0 binning scheme, and 0.0034 using the B^0_s binning scheme. These values are assigned as systematic uncertainties for $A_P(B^0)$ and $A_P(B^0_s)$. Table 6 summarizes the systematic uncertainties associated with the integrated measurements. In the first row, the combined systematic uncertainties estimated in each bin, as described in the previous section, are reported.

Using Eq. (9), the integrated measurements of $A_P(B^0)$ for $B^0 \to J/\psi K^{*0}$ and $B^0 \to D^-\pi^+$ decays are found to be

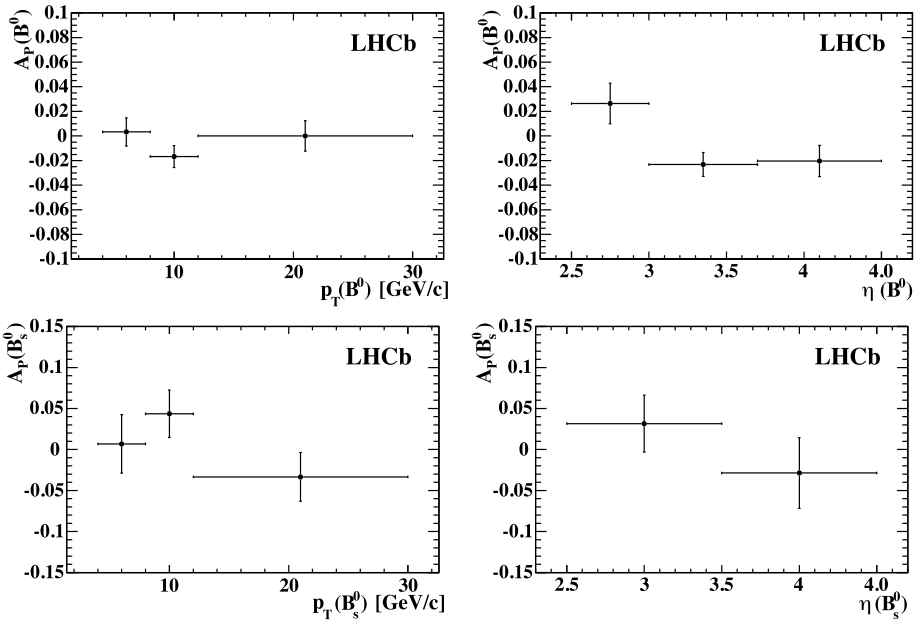

Fig. 4. Dependence of (top) $A_P(B^0)$ and (bottom) $A_P(B_s^0)$ on (left) p_T and (right) η. The error bars include both statistical and systematic uncertainties.

Table 6
Absolute values of systematic uncertainties. The total systematic uncertainties are obtained by summing the individual contributions in quadrature.

Source	Uncertainty	
	$A_P(B^0)$	$A_P(B_s^0)$
Combined systematic uncertainties from bin studies	0.0004	0.0048
Uncertainty on $\lvert q/p\rvert$	0.0013	0.0030
Difference between ω_i and ω_i^{data}	0.0024	0.0034
Total	0.0028	0.0066

Table 7
Values of the production asymmetry $A_P(B^0)$ in bins of p_T and η from $B^0 \to J/\psi K^{*0}$ and $B^0 \to D^-\pi^+$ decays. The first uncertainties are statistical and the second systematic.

Variable	Bin	$A_P(B^0)$
p_T (GeV/c)	(4, 7)	$0.0033 \pm 0.0111 \pm 0.0028$
	(7, 12)	$-0.0167 \pm 0.0084 \pm 0.0028$
	(12, 30)	$0.0001 \pm 0.0130 \pm 0.0029$
η	(2.5, 3.0)	$0.0264 \pm 0.0161 \pm 0.0030$
	(3.0, 3.7)	$-0.0232 \pm 0.0093 \pm 0.0028$
	(3.7, 4.5)	$-0.0203 \pm 0.0125 \pm 0.0021$

$$A_P\left(B^0 \to J/\psi K^{*0}\right) = -0.0033 \pm 0.0096\ (\text{stat}) \pm 0.0028\ (\text{syst}),$$

$$A_P\left(B^0 \to D^-\pi^+\right) = -0.0038 \pm 0.0124\ (\text{stat}) \pm 0.0029\ (\text{syst}),$$

which lead to the average

$$A_P\left(B^0\right) = -0.0035 \pm 0.0076\ (\text{stat}) \pm 0.0028\ (\text{syst}).$$

The integrated value of $A_P(B_s^0)$ is

$$A_P\left(B_s^0\right) = 0.0109 \pm 0.0261\ (\text{stat}) \pm 0.0066\ (\text{syst}).$$

Finally, the dependencies of $A_P(B^0)$ and $A_P(B_s^0)$ on p_T, obtained by integrating over η, and on η, obtained by integrating over p_T, are shown in Fig. 4. The corresponding numerical values are reported in Tables 7 and 8.

Table 8
Values of the production asymmetry $A_P(B_s^0)$ in bins of p_T and η from $B_s^0 \to D_s^-\pi^+$ decays. The first uncertainties are statistical and the second systematic.

Variable	Bin	$A_P(B_s^0)$
p_T (GeV/c)	(4, 8)	$0.0069 \pm 0.0351 \pm 0.0067$
	(8, 12)	$0.0435 \pm 0.0283 \pm 0.0039$
	(12, 30)	$-0.0334 \pm 0.0296 \pm 0.0038$
η	(2.5, 3.5)	$0.0315 \pm 0.0342 \pm 0.0060$
	(3.5, 4.5)	$-0.0286 \pm 0.0412 \pm 0.0088$

8. Conclusions

The production asymmetries of B^0 and B_s^0 mesons have been measured in pp collisions at $\sqrt{s} = 7$ TeV within the acceptance of the LHCb detector, using a data sample corresponding to an integrated luminosity of 1.0 fb^{-1}. The measurements have been performed in bins of p_T and η, and provide constraints that can be used to test different models of B-meson production. Furthermore, once integrated using appropriate weights for any reconstructed $B_{(s)}^0$ decay mode, they can be used to derive effective production asymmetries, as inputs for CP violation measurements with the LHCb detector.

The values of the production asymmetries integrated in the ranges $4 < p_T < 30$ GeV/c and $2.5 < \eta < 4.5$ have been determined to be

$$A_P\left(B^0\right) = (-0.35 \pm 0.76 \pm 0.28)\%,$$

$$A_P\left(B_s^0\right) = (1.09 \pm 2.61 \pm 0.66)\%,$$

where the first uncertainties are statistical and the second systematic. No clear evidence of dependences on the values of p_T and η has been observed.

Acknowledgements

We express our gratitude to our colleagues in the CERN accelerator departments for the excellent performance of the LHC. We thank the technical and administrative staff at the LHCb institutes. We acknowledge support from CERN and from the national

agencies: CAPES, CNPq, FAPERJ and FINEP (Brazil); NSFC (China); CNRS/IN2P3 (France); BMBF, DFG, HGF and MPG (Germany); SFI (Ireland); INFN (Italy); FOM and NWO (The Netherlands); MNiSW and NCN (Poland); MEN/IFA (Romania); MinES and FANO (Russia); MinECo (Spain); SNSF and SER (Switzerland); NASU (Ukraine); STFC (United Kingdom); NSF (USA). The Tier1 computing centres are supported by IN2P3 (France), KIT and BMBF (Germany), INFN (Italy), NWO and SURF (The Netherlands), PIC (Spain), GridPP (United Kingdom). We are indebted to the communities behind the multiple open source software packages on which we depend. We are also thankful for the computing resources and the access to software R&D tools provided by Yandex LLC (Russia). Individual groups or members have received support from EPLANET, Marie Skłodowska-Curie Actions and ERC (European Union), Conseil général de Haute-Savoie, Labex ENIGMASS and OCEVU, Région Auvergne (France), RFBR (Russia), XuntaGal and GENCAT (Spain), Royal Society and Royal Commission for the Exhibition of 1851 (United Kingdom).

References

[1] M. Chaichian, A. Fridman, On a possibility for measuring effects of CP violation at pp colliders, Phys. Lett. B 298 (1993) 218.
[2] E. Norrbin, R. Vogt, Bottom production asymmetries at the LHC, arXiv:hep-ph/0003056.
[3] E. Norrbin, T. Sjöstrand, Production and hadronization of heavy quarks, Eur. Phys. J. C 17 (2000) 137, arXiv:hep-ph/0005110.
[4] LHCb Collaboration, R. Aaij, et al., Measurement of the $D^{\pm}$ production asymmetry in 7 TeV pp collisions, Phys. Lett. B 718 (2013) 902, arXiv:1210.4112.
[5] LHCb Collaboration, R. Aaij, et al., Measurement of the $D_s^+ - D_s^-$ production asymmetry in 7 TeV pp collisions, Phys. Lett. B 713 (2012) 186, arXiv:1205.0897.
[6] LHCb Collaboration, A.A. Alves Jr., et al., The LHCb detector at the LHC, J. Instrum. 3 (2008) S08005.
[7] Particle Data Group, J. Beringer, et al., Review of particle physics, Phys. Rev. D 86 (2012) 010001, and 2013 partial update for the 2014 edition.
[8] V.V. Gligorov, M. Williams, Efficient, reliable and fast high-level triggering using a bonsai boosted decision tree, J. Instrum. 8 (2013) P02013, arXiv:1210.6861.
[9] T. Sjöstrand, S. Mrenna, P. Skands, PYTHIA 6.4 physics and manual, J. High Energy Phys. 05 (2006) 026, arXiv:hep-ph/0603175.
[10] I. Belyaev, et al., Handling of the generation of primary events in Gauss, the LHCb simulation framework, in: Nuclear Science Symposium Conference Record, NSS/MIC, IEEE, 2010, p. 1155.
[11] GEANT4 Collaboration, J. Allison, et al., Geant4 developments and applications, IEEE Trans. Nucl. Sci. 53 (2006) 270;
GEANT4 Collaboration, S. Agostinelli, et al., GEANT4: a simulation toolkit, Nucl. Instrum. Methods, Sect. A 506 (2003) 250.
[12] M. Clemencic, et al., The LHCb simulation application, Gauss: design, evolution and experience, J. Phys. Conf. Ser. 331 (2011) 032023.
[13] W.D. Hulsbergen, Decay chain fitting with a Kalman filter, Nucl. Instrum. Methods, Sect. A 552 (2005) 566, arXiv:physics/0503191.
[14] L. Breiman, J.H. Friedman, R.A. Olshen, C.J. Stone, Classification and Regression Trees, Wadsworth International Group, Belmont, California, USA, 1984.
[15] R.E. Schapire, Y. Freund, A decision-theoretic generalization of on-line learning and an application to boosting, J. Comput. Syst. Sci. 55 (1997) 119.
[16] K.S. Cranmer, Kernel estimation in high-energy physics, Comput. Phys. Commun. 136 (2001) 198, arXiv:hep-ex/0011057.
[17] LHCb Collaboration, R. Aaij, et al., Measurement of the fragmentation fraction ratio f_s/f_d and its dependence on B meson kinematics, J. High Energy Phys. 04 (2013) 001, arXiv:1301.5286.
[18] LHCb Collaboration, R. Aaij, et al., Measurement of b hadron production fractions in 7 TeV pp collisions, Phys. Rev. D 85 (2012) 032008, arXiv:1111.2357.
[19] LHCb Collaboration, R. Aaij, et al., Precision measurement of the B_s^0–$\bar{B}_s^0$ oscillation frequency with the decay $B_s^0 \to D_s^- \pi^+$, New J. Phys. 15 (2013) 053021, arXiv:1304.4741.
[20] Heavy Flavor Averaging Group, Y. Amhis, et al., Averages of b-hadron, c-hadron, and τ-lepton properties as of early 2012, arXiv:1207.1158, update available online at http://www.slac.stanford.edu/xorg/hfag.
[21] LHCb Collaboration, R. Aaij, et al., Measurement of the flavour-specific CP-violating asymmetry $a_{\rm sl}^s$ in B_s^0 decays, Phys. Lett. B 728 (2014) 607, arXiv:1308.1048.
[22] M. Pivk, F.R. Le Diberder, sPlot: a statistical tool to unfold data distributions, Nucl. Instrum. Methods, Sect. A 555 (2005) 356, arXiv:physics/0402083.

LHCb Collaboration

R. Aaij [41], B. Adeva [37], M. Adinolfi [46], A. Affolder [52], Z. Ajaltouni [5], S. Akar [6], J. Albrecht [9], F. Alessio [38], M. Alexander [51], S. Ali [41], G. Alkhazov [30], P. Alvarez Cartelle [37], A.A. Alves Jr. [25,38], S. Amato [2], S. Amerio [22], Y. Amhis [7], L. An [3], L. Anderlini [17,g], J. Anderson [40], R. Andreassen [57], M. Andreotti [16,f], J.E. Andrews [58], R.B. Appleby [54], O. Aquines Gutierrez [10], F. Archilli [38], A. Artamonov [35], M. Artuso [59], E. Aslanides [6], G. Auriemma [25,n], M. Baalouch [5], S. Bachmann [11], J.J. Back [48], A. Badalov [36], W. Baldini [16], R.J. Barlow [54], C. Barschel [38], S. Barsuk [7], W. Barter [47], V. Batozskaya [28], V. Battista [39], A. Bay [39], L. Beaucourt [4], J. Beddow [51], F. Bedeschi [23], I. Bediaga [1], S. Belogurov [31], K. Belous [35], I. Belyaev [31], E. Ben-Haim [8], G. Bencivenni [18], S. Benson [38], J. Benton [46], A. Berezhnoy [32], R. Bernet [40], M.-O. Bettler [47], M. van Beuzekom [41], A. Bien [11], S. Bifani [45], T. Bird [54], A. Bizzeti [17,i], P.M. Bjørnstad [54], T. Blake [48], F. Blanc [39], J. Blouw [10], S. Blusk [59], V. Bocci [25], A. Bondar [34], N. Bondar [30,38], W. Bonivento [15,38], S. Borghi [54], A. Borgia [59], M. Borsato [7], T.J.V. Bowcock [52], E. Bowen [40], C. Bozzi [16], T. Brambach [9], J. van den Brand [42], J. Bressieux [39], D. Brett [54], M. Britsch [10], T. Britton [59], J. Brodzicka [54], N.H. Brook [46], H. Brown [52], A. Bursche [40], G. Busetto [22,r], J. Buytaert [38], S. Cadeddu [15], R. Calabrese [16,f], M. Calvi [20,k], M. Calvo Gomez [36,p], P. Campana [18,38], D. Campora Perez [38], A. Carbone [14,d], G. Carboni [24,l], R. Cardinale [19,38,j], A. Cardini [15], L. Carson [50], K. Carvalho Akiba [2], G. Casse [52], L. Cassina [20], L. Castillo Garcia [38], M. Cattaneo [38], Ch. Cauet [9], R. Cenci [58], M. Charles [8], Ph. Charpentier [38], M. Chefdeville [4], S. Chen [54], S.-F. Cheung [55], N. Chiapolini [40], M. Chrzaszcz [40,26], K. Ciba [38], X. Cid Vidal [38], G. Ciezarek [53], P.E.L. Clarke [50], M. Clemencic [38], H.V. Cliff [47], J. Closier [38], V. Coco [38], J. Cogan [6], E. Cogneras [5], L. Cojocariu [29], P. Collins [38], A. Comerma-Montells [11], A. Contu [15], A. Cook [46], M. Coombes [46], S. Coquereau [8], G. Corti [38], M. Corvo [16,f], I. Counts [56], B. Couturier [38], G.A. Cowan [50], D.C. Craik [48], M. Cruz Torres [60], S. Cunliffe [53], R. Currie [50], C. D'Ambrosio [38], J. Dalseno [46], P. David [8], P.N.Y. David [41], A. Davis [57], K. De Bruyn [41], S. De Capua [54], M. De Cian [11], J.M. De Miranda [1], L. De Paula [2], W. De Silva [57], P. De Simone [18], D. Decamp [4], M. Deckenhoff [9], L. Del Buono [8], N. Déléage [4], D. Derkach [55],

O. Deschamps [5], F. Dettori [38], A. Di Canto [38], H. Dijkstra [38], S. Donleavy [52], F. Dordei [11], M. Dorigo [39], A. Dosil Suárez [37], D. Dossett [48], A. Dovbnya [43], K. Dreimanis [52], G. Dujany [54], F. Dupertuis [39], P. Durante [38], R. Dzhelyadin [35], A. Dziurda [26], A. Dzyuba [30], S. Easo [49,38], U. Egede [53], V. Egorychev [31], S. Eidelman [34], S. Eisenhardt [50], U. Eitschberger [9], R. Ekelhof [9], L. Eklund [51], I. El Rifai [5], Ch. Elsasser [40], S. Ely [59], S. Esen [11], H.-M. Evans [47], T. Evans [55], A. Falabella [14], C. Färber [11], C. Farinelli [41], N. Farley [45], S. Farry [52], R.F. Fay [52], D. Ferguson [50], V. Fernandez Albor [37], F. Ferreira Rodrigues [1], M. Ferro-Luzzi [38], S. Filippov [33], M. Fiore [16,f], M. Fiorini [16,f], M. Firlej [27], C. Fitzpatrick [39], T. Fiutowski [27], M. Fontana [10], F. Fontanelli [19,j], R. Forty [38], O. Francisco [2], M. Frank [38], C. Frei [38], M. Frosini [17,38,g], J. Fu [21,38], E. Furfaro [24,l], A. Gallas Torreira [37], D. Galli [14,d], S. Gallorini [22], S. Gambetta [19,j], M. Gandelman [2], P. Gandini [59], Y. Gao [3], J. García Pardiñas [37], J. Garofoli [59], J. Garra Tico [47], L. Garrido [36], C. Gaspar [38], R. Gauld [55], L. Gavardi [9], G. Gavrilov [30], A. Geraci [21,v], E. Gersabeck [11], M. Gersabeck [54], T. Gershon [48], Ph. Ghez [4], A. Gianelle [22], S. Giani' [39], V. Gibson [47], L. Giubega [29], V.V. Gligorov [38], C. Göbel [60], D. Golubkov [31], A. Golutvin [53,31,38], A. Gomes [1,a], C. Gotti [20], M. Grabalosa Gándara [5], R. Graciani Diaz [36], L.A. Granado Cardoso [38], E. Graugés [36], G. Graziani [17], A. Grecu [29], E. Greening [55], S. Gregson [47], P. Griffith [45], L. Grillo [11], O. Grünberg [62], B. Gui [59], E. Gushchin [33], Yu. Guz [35,38], T. Gys [38], C. Hadjivasiliou [59], G. Haefeli [39], C. Haen [38], S.C. Haines [47], S. Hall [53], B. Hamilton [58], T. Hampson [46], X. Han [11], S. Hansmann-Menzemer [11], N. Harnew [55], S.T. Harnew [46], J. Harrison [54], J. He [38], T. Head [38], V. Heijne [41], K. Hennessy [52], P. Henrard [5], L. Henry [8], J.A. Hernando Morata [37], E. van Herwijnen [38], M. Heß [62], A. Hicheur [1], D. Hill [55], M. Hoballah [5], C. Hombach [54], W. Hulsbergen [41], P. Hunt [55], N. Hussain [55], D. Hutchcroft [52], D. Hynds [51], M. Idzik [27], P. Ilten [56], R. Jacobsson [38], A. Jaeger [11], J. Jalocha [55], E. Jans [41], P. Jaton [39], A. Jawahery [58], F. Jing [3], M. John [55], D. Johnson [55], C.R. Jones [47], C. Joram [38], B. Jost [38], N. Jurik [59], M. Kaballo [9], S. Kandybei [43], W. Kanso [6], M. Karacson [38], T.M. Karbach [38], S. Karodia [51], M. Kelsey [59], I.R. Kenyon [45], T. Ketel [42], B. Khanji [20], C. Khurewathanakul [39], S. Klaver [54], K. Klimaszewski [28], O. Kochebina [7], M. Kolpin [11], I. Komarov [39], R.F. Koopman [42], P. Koppenburg [41,38], M. Korolev [32], A. Kozlinskiy [41], L. Kravchuk [33], K. Kreplin [11], M. Kreps [48], G. Krocker [11], P. Krokovny [34], F. Kruse [9], W. Kucewicz [26,o], M. Kucharczyk [20,26,38,k], V. Kudryavtsev [34], K. Kurek [28], T. Kvaratskheliya [31], V.N. La Thi [39], D. Lacarrere [38], G. Lafferty [54], A. Lai [15], D. Lambert [50], R.W. Lambert [42], G. Lanfranchi [18], C. Langenbruch [48], B. Langhans [38], T. Latham [48], C. Lazzeroni [45], R. Le Gac [6], J. van Leerdam [41], J.-P. Lees [4], R. Lefèvre [5], A. Leflat [32], J. Lefrançois [7], S. Leo [23], O. Leroy [6], T. Lesiak [26], B. Leverington [11], Y. Li [3], T. Likhomanenko [63], M. Liles [52], R. Lindner [38], C. Linn [38], F. Lionetto [40], B. Liu [15], S. Lohn [38], I. Longstaff [51], J.H. Lopes [2], N. Lopez-March [39], P. Lowdon [40], H. Lu [3], D. Lucchesi [22,r], H. Luo [50], A. Lupato [22], E. Luppi [16,f], O. Lupton [55], F. Machefert [7], I.V. Machikhiliyan [31], F. Maciuc [29], O. Maev [30], S. Malde [55], A. Malinin [63], G. Manca [15,e], G. Mancinelli [6], A. Mapelli [38], J. Maratas [5], J.F. Marchand [4], U. Marconi [14], C. Marin Benito [36], P. Marino [23,t], R. Märki [39], J. Marks [11], G. Martellotti [25], A. Martens [8], A. Martín Sánchez [7], M. Martinelli [39], D. Martinez Santos [42], F. Martinez Vidal [64], D. Martins Tostes [2], A. Massafferri [1], R. Matev [38], Z. Mathe [38], C. Matteuzzi [20], A. Mazurov [16,f], M. McCann [53], J. McCarthy [45], A. McNab [54], R. McNulty [12], B. McSkelly [52], B. Meadows [57], F. Meier [9], M. Meissner [11], M. Merk [41], D.A. Milanes [8], M.-N. Minard [4], N. Moggi [14], J. Molina Rodriguez [60], S. Monteil [5], M. Morandin [22], P. Morawski [27], A. Mordà [6], M.J. Morello [23,t], J. Moron [27], A.-B. Morris [50], R. Mountain [59], F. Muheim [50], K. Müller [40], M. Mussini [14], B. Muster [39], P. Naik [46], T. Nakada [39], R. Nandakumar [49], I. Nasteva [2], M. Needham [50], N. Neri [21], S. Neubert [38], N. Neufeld [38], M. Neuner [11], A.D. Nguyen [39], T.D. Nguyen [39], C. Nguyen-Mau [39,q], M. Nicol [7], V. Niess [5], R. Niet [9], N. Nikitin [32], T. Nikodem [11], A. Novoselov [35], D.P. O'Hanlon [48], A. Oblakowska-Mucha [27], V. Obraztsov [35], S. Oggero [41], S. Ogilvy [51], O. Okhrimenko [44], R. Oldeman [15,e], G. Onderwater [65], M. Orlandea [29], J.M. Otalora Goicochea [2], P. Owen [53], A. Oyanguren [64], B.K. Pal [59], A. Palano [13,c], F. Palombo [21,u], M. Palutan [18], J. Panman [38], A. Papanestis [49,38], M. Pappagallo [51], L.L. Pappalardo [16,f], C. Parkes [54], C.J. Parkinson [9,45], G. Passaleva [17], G.D. Patel [52], M. Patel [53], C. Patrignani [19,j], A. Pazos Alvarez [37], A. Pearce [54], A. Pellegrino [41], M. Pepe Altarelli [38], S. Perazzini [14,d], E. Perez Trigo [37], P. Perret [5], M. Perrin-Terrin [6], L. Pescatore [45], E. Pesen [66], K. Petridis [53], A. Petrolini [19,j], E. Picatoste Olloqui [36], B. Pietrzyk [4], T. Pilař [48], D. Pinci [25], A. Pistone [19], S. Playfer [50], M. Plo Casasus [37], F. Polci [8], A. Poluektov [48,34], E. Polycarpo [2], A. Popov [35], D. Popov [10], B. Popovici [29], C. Potterat [2], E. Price [46], J. Prisciandaro [39], A. Pritchard [52], C. Prouve [46], V. Pugatch [44], A. Puig Navarro [39], G. Punzi [23,s], W. Qian [4], B. Rachwal [26], J.H. Rademacker [46], B. Rakotomiaramanana [39], M. Rama [18], M.S. Rangel [2],

I. Raniuk [43], N. Rauschmayr [38], G. Raven [42], S. Reichert [54], M.M. Reid [48], A.C. dos Reis [1], S. Ricciardi [49], S. Richards [46], M. Rihl [38], K. Rinnert [52], V. Rives Molina [36], D.A. Roa Romero [5], P. Robbe [7], A.B. Rodrigues [1], E. Rodrigues [54], P. Rodriguez Perez [54], S. Roiser [38], V. Romanovsky [35], A. Romero Vidal [37], M. Rotondo [22], J. Rouvinet [39], T. Ruf [38], H. Ruiz [36], P. Ruiz Valls [64], J.J. Saborido Silva [37], N. Sagidova [30], P. Sail [51], B. Saitta [15,e], V. Salustino Guimaraes [2], C. Sanchez Mayordomo [64], B. Sanmartin Sedes [37], R. Santacesaria [25], C. Santamarina Rios [37], E. Santovetti [24,l], A. Sarti [18,m], C. Satriano [25,n], A. Satta [24], D.M. Saunders [46], M. Savrie [16,f], D. Savrina [31,32], M. Schiller [42], H. Schindler [38], M. Schlupp [9], M. Schmelling [10], B. Schmidt [38], O. Schneider [39], A. Schopper [38], M.-H. Schune [7], R. Schwemmer [38], B. Sciascia [18], A. Sciubba [25], M. Seco [37], A. Semennikov [31], I. Sepp [53], N. Serra [40], J. Serrano [6], L. Sestini [22], P. Seyfert [11], M. Shapkin [35], I. Shapoval [16,43,f], Y. Shcheglov [30], T. Shears [52], L. Shekhtman [34], V. Shevchenko [63], A. Shires [9], R. Silva Coutinho [48], G. Simi [22], M. Sirendi [47], N. Skidmore [46], T. Skwarnicki [59], N.A. Smith [52], E. Smith [55,49], E. Smith [53], J. Smith [47], M. Smith [54], H. Snoek [41], M.D. Sokoloff [57], F.J.P. Soler [51], F. Soomro [39], D. Souza [46], B. Souza De Paula [2], B. Spaan [9], A. Sparkes [50], P. Spradlin [51], S. Sridharan [38], F. Stagni [38], M. Stahl [11], S. Stahl [11], O. Steinkamp [40], O. Stenyakin [35], S. Stevenson [55], S. Stoica [29], S. Stone [59], B. Storaci [40], S. Stracka [23,38], M. Straticiuc [29], U. Straumann [40], R. Stroili [22], V.K. Subbiah [38], L. Sun [57], W. Sutcliffe [53], K. Swientek [27], S. Swientek [9], V. Syropoulos [42], M. Szczekowski [28], P. Szczypka [39,38], D. Szilard [2], T. Szumlak [27], S. T'Jampens [4], M. Teklishyn [7], G. Tellarini [16,f], F. Teubert [38], C. Thomas [55], E. Thomas [38], J. van Tilburg [41], V. Tisserand [4], M. Tobin [39], S. Tolk [42], L. Tomassetti [16,f], D. Tonelli [38], S. Topp-Joergensen [55], N. Torr [55], E. Tournefier [4], S. Tourneur [39], M.T. Tran [39], M. Tresch [40], A. Tsaregorodtsev [6], P. Tsopelas [41], N. Tuning [41], M. Ubeda Garcia [38], A. Ukleja [28], A. Ustyuzhanin [63], U. Uwer [11], V. Vagnoni [14,*], G. Valenti [14], A. Vallier [7], R. Vazquez Gomez [18], P. Vazquez Regueiro [37], C. Vázquez Sierra [37], S. Vecchi [16], J.J. Velthuis [46], M. Veltri [17,h], G. Veneziano [39], M. Vesterinen [11], B. Viaud [7], D. Vieira [2], M. Vieites Diaz [37], X. Vilasis-Cardona [36,p], A. Vollhardt [40], D. Volyanskyy [10], D. Voong [46], A. Vorobyev [30], V. Vorobyev [34], C. Voß [62], H. Voss [10], J.A. de Vries [41], R. Waldi [62], C. Wallace [48], R. Wallace [12], J. Walsh [23], S. Wandernoth [11], J. Wang [59], D.R. Ward [47], N.K. Watson [45], D. Websdale [53], M. Whitehead [48], J. Wicht [38], D. Wiedner [11], G. Wilkinson [55], M.P. Williams [45], M. Williams [56], F.F. Wilson [49], J. Wimberley [58], J. Wishahi [9], W. Wislicki [28], M. Witek [26], G. Wormser [7], S.A. Wotton [47], S. Wright [47], S. Wu [3], K. Wyllie [38], Y. Xie [61], Z. Xing [59], Z. Xu [39], Z. Yang [3], X. Yuan [3], O. Yushchenko [35], M. Zangoli [14], M. Zavertyaev [10,b], L. Zhang [59], W.C. Zhang [12], Y. Zhang [3], A. Zhelezov [11], A. Zhokhov [31], L. Zhong [3], A. Zvyagin [38]

[1] *Centro Brasileiro de Pesquisas Físicas (CBPF), Rio de Janeiro, Brazil*
[2] *Universidade Federal do Rio de Janeiro (UFRJ), Rio de Janeiro, Brazil*
[3] *Center for High Energy Physics, Tsinghua University, Beijing, China*
[4] *LAPP, Université de Savoie, CNRS/IN2P3, Annecy-Le-Vieux, France*
[5] *Clermont Université, Université Blaise Pascal, CNRS/IN2P3, LPC, Clermont-Ferrand, France*
[6] *CPPM, Aix-Marseille Université, CNRS/IN2P3, Marseille, France*
[7] *LAL, Université Paris-Sud, CNRS/IN2P3, Orsay, France*
[8] *LPNHE, Université Pierre et Marie Curie, Université Paris Diderot, CNRS/IN2P3, Paris, France*
[9] *Fakultät Physik, Technische Universität Dortmund, Dortmund, Germany*
[10] *Max-Planck-Institut für Kernphysik (MPIK), Heidelberg, Germany*
[11] *Physikalisches Institut, Ruprecht-Karls-Universität Heidelberg, Heidelberg, Germany*
[12] *School of Physics, University College Dublin, Dublin, Ireland*
[13] *Sezione INFN di Bari, Bari, Italy*
[14] *Sezione INFN di Bologna, Bologna, Italy*
[15] *Sezione INFN di Cagliari, Cagliari, Italy*
[16] *Sezione INFN di Ferrara, Ferrara, Italy*
[17] *Sezione INFN di Firenze, Firenze, Italy*
[18] *Laboratori Nazionali dell'INFN di Frascati, Frascati, Italy*
[19] *Sezione INFN di Genova, Genova, Italy*
[20] *Sezione INFN di Milano Bicocca, Milano, Italy*
[21] *Sezione INFN di Milano, Milano, Italy*
[22] *Sezione INFN di Padova, Padova, Italy*
[23] *Sezione INFN di Pisa, Pisa, Italy*
[24] *Sezione INFN di Roma Tor Vergata, Roma, Italy*
[25] *Sezione INFN di Roma La Sapienza, Roma, Italy*
[26] *Henryk Niewodniczanski Institute of Nuclear Physics Polish Academy of Sciences, Kraków, Poland*
[27] *AGH – University of Science and Technology, Faculty of Physics and Applied Computer Science, Kraków, Poland*
[28] *National Center for Nuclear Research (NCBJ), Warsaw, Poland*
[29] *Horia Hulubei National Institute of Physics and Nuclear Engineering, Bucharest-Magurele, Romania*
[30] *Petersburg Nuclear Physics Institute (PNPI), Gatchina, Russia*
[31] *Institute of Theoretical and Experimental Physics (ITEP), Moscow, Russia*
[32] *Institute of Nuclear Physics, Moscow State University (SINP MSU), Moscow, Russia*
[33] *Institute for Nuclear Research of the Russian Academy of Sciences (INR RAN), Moscow, Russia*

[34] Budker Institute of Nuclear Physics (SB RAS) and Novosibirsk State University, Novosibirsk, Russia
[35] Institute for High Energy Physics (IHEP), Protvino, Russia
[36] Universitat de Barcelona, Barcelona, Spain
[37] Universidad de Santiago de Compostela, Santiago de Compostela, Spain
[38] European Organization for Nuclear Research (CERN), Geneva, Switzerland
[39] Ecole Polytechnique Fédérale de Lausanne (EPFL), Lausanne, Switzerland
[40] Physik-Institut, Universität Zürich, Zürich, Switzerland
[41] Nikhef National Institute for Subatomic Physics, Amsterdam, The Netherlands
[42] Nikhef National Institute for Subatomic Physics and VU University Amsterdam, Amsterdam, The Netherlands
[43] NSC Kharkiv Institute of Physics and Technology (NSC KIPT), Kharkiv, Ukraine
[44] Institute for Nuclear Research of the National Academy of Sciences (KINR), Kyiv, Ukraine
[45] University of Birmingham, Birmingham, United Kingdom
[46] H.H. Wills Physics Laboratory, University of Bristol, Bristol, United Kingdom
[47] Cavendish Laboratory, University of Cambridge, Cambridge, United Kingdom
[48] Department of Physics, University of Warwick, Coventry, United Kingdom
[49] STFC Rutherford Appleton Laboratory, Didcot, United Kingdom
[50] School of Physics and Astronomy, University of Edinburgh, Edinburgh, United Kingdom
[51] School of Physics and Astronomy, University of Glasgow, Glasgow, United Kingdom
[52] Oliver Lodge Laboratory, University of Liverpool, Liverpool, United Kingdom
[53] Imperial College London, London, United Kingdom
[54] School of Physics and Astronomy, University of Manchester, Manchester, United Kingdom
[55] Department of Physics, University of Oxford, Oxford, United Kingdom
[56] Massachusetts Institute of Technology, Cambridge, MA, United States
[57] University of Cincinnati, Cincinnati, OH, United States
[58] University of Maryland, College Park, MD, United States
[59] Syracuse University, Syracuse, NY, United States
[60] Pontifícia Universidade Católica do Rio de Janeiro (PUC-Rio), Rio de Janeiro, Brazil [w]
[61] Institute of Particle Physics, Central China Normal University, Wuhan, Hubei, China [x]
[62] Institut für Physik, Universität Rostock, Rostock, Germany [y]
[63] National Research Centre Kurchatov Institute, Moscow, Russia [z]
[64] Instituto de Fisica Corpuscular (IFIC), Universitat de Valencia-CSIC, Valencia, Spain [aa]
[65] KVI – University of Groningen, Groningen, The Netherlands [ab]
[66] Celal Bayar University, Manisa, Turkey [ac]

* Corresponding author.
E-mail address: Vincenzo.Vagnoni@bo.infn.it (V. Vagnoni).
[a] Universidade Federal do Triângulo Mineiro (UFTM), Uberaba-MG, Brazil.
[b] P.N. Lebedev Physical Institute, Russian Academy of Science (LPI RAS), Moscow, Russia.
[c] Università di Bari, Bari, Italy.
[d] Università di Bologna, Bologna, Italy.
[e] Università di Cagliari, Cagliari, Italy.
[f] Università di Ferrara, Ferrara, Italy.
[g] Università di Firenze, Firenze, Italy.
[h] Università di Urbino, Urbino, Italy.
[i] Università di Modena e Reggio Emilia, Modena, Italy.
[j] Università di Genova, Genova, Italy.
[k] Università di Milano Bicocca, Milano, Italy.
[l] Università di Roma Tor Vergata, Roma, Italy.
[m] Università di Roma La Sapienza, Roma, Italy.
[n] Università della Basilicata, Potenza, Italy.
[o] AGH – University of Science and Technology, Faculty of Computer Science, Electronics and Telecommunications, Kraków, Poland.
[p] LIFAELS, La Salle, Universitat Ramon Llull, Barcelona, Spain.
[q] Hanoi University of Science, Hanoi, Viet Nam.
[r] Università di Padova, Padova, Italy.
[s] Università di Pisa, Pisa, Italy.
[t] Scuola Normale Superiore, Pisa, Italy.
[u] Università degli Studi di Milano, Milano, Italy.
[v] Politecnico di Milano, Milano, Italy.
[w] Associated to Universidade Federal do Rio de Janeiro (UFRJ), Rio de Janeiro, Brazil.
[x] Associated to Center for High Energy Physics, Tsinghua University, Beijing, China.
[y] Associated to Physikalisches Institut, Ruprecht-Karls-Universität Heidelberg, Heidelberg, Germany.
[z] Associated to Institute of Theoretical and Experimental Physics (ITEP), Moscow, Russia.
[aa] Associated to Universitat de Barcelona, Barcelona, Spain.
[ab] Associated to Nikhef National Institute for Subatomic Physics, Amsterdam, The Netherlands.
[ac] Associated to European Organization for Nuclear Research (CERN), Geneva, Switzerland.